Quenching the Anisotropic Heisenberg Chain: Exact Solution and Generalized Gibbs Ensemble Predictions

Wouters, B.; De Nardis, J.; Brockmann, M.; Fioretto, D.; Rigol, M.; Caux, J.-S.

Published in:
Physical Review Letters

DOI:
10.1103/PhysRevLett.113.117202

Quenching the Anisotropic Heisenberg Chain: Exact Solution and Generalized Gibbs Ensemble Predictions

B. Wouters,[1] J. De Nardis,[1] M. Brockmann,[1] D. Fioretto,[1] M. Rigol,[2] and J.-S. Caux[1]
[1]Institute for Theoretical Physics, University of Amsterdam, Science Park 904, Postbus 94485, 1090 GL Amsterdam, Netherlands
[2]Department of Physics, The Pennsylvania State University, University Park, Pennsylvania 16802, USA
(Received 15 May 2014; revised manuscript received 22 July 2014; published 9 September 2014)

We study quenches in integrable spin-1/2 chains in which we evolve the ground state of the antiferromagnetic Ising model with the anisotropic Heisenberg Hamiltonian. For this nontrivially interacting situation, an application of the first-principles-based quench-action method allows us to give an exact description of the postquench steady state in the thermodynamic limit. We show that a generalized Gibbs ensemble, implemented using all known local conserved charges, fails to reproduce the exact quench-action steady state and to correctly predict postquench equilibrium expectation values of physical observables. This is supported by numerical linked-cluster calculations within the diagonal ensemble in the thermodynamic limit.

DOI: 10.1103/PhysRevLett.113.117202 PACS numbers: 75.10.Jm, 02.30.Ik, 05.70.Ln

Introduction.—Out-of-equilibrium phenomena are of importance throughout physics, in fields ranging from cosmology [1] and superfluid helium [2], heavy-ion collisions [3], pattern formation [4], exclusion processes [5], and glasses [6] all the way to atomic-scale isolated quantum systems [7]. Much recent experimental and theoretical activity has been focused on the latter, raising fundamental questions as to whether, how, and to what state such systems relax under unitary time evolution following a sudden quantum quench [8–42]. From this work, two scenarios for equilibration have emerged, one applicable to models having only a few local conserved quantities, the other relevant to integrable models characterized by an infinite number of local conserved charges. In the former, thermalization to a Gibbs ensemble is the rule [11], while in the latter, equilibration to a so-called generalized Gibbs ensemble (GGE) [9,10] is generally thought to occur, in particular for lattice spin systems [12–20].

In this Letter, we study a quench in which the second scenario breaks down. Our initial state, defined as a purely antiferromagnetic (spin-1/2 Néel) state, is let to evolve unitarily in time according to the XXZ spin chain Hamiltonian. This is a physically meaningful quench protocol, which can, in principle, be implemented using cold atoms [43–47]. We provide a thermodynamically exact solution for the steady state reached long after the quench, derived directly from microscopics using the recently proposed quench-action method [48]. The solution takes the form of a set of distributions of quasimomenta that completely characterizes the macrostate representing the steady state, from which observables of interest can be calculated. As a stringent test, it correctly reproduces the expectation values of all local conserved charges. Furthermore, we implement a numerical linked-cluster expansion (NLCE) [49,50] whose results support the correctness of the quench-action approach. Our application of the latter to nontrivially interacting lattice models follows up on the recent quench-action solution of interaction quenches in one-dimensional Bose systems [51] and demonstrates the broad applicability of the approach.

Besides providing the exact solution using the quench action, we explicitly construct a GGE for the Néel-to-XXZ quench using all known local conserved charges, enabling an analytical check of the GGE logic applied to interacting systems. We show that it fails to reproduce the steady state as predicted by the quench action. As a consequence, equilibrium expectation values of physical observables are predicted differently by the quench-action method, which corresponds to the prediction of the diagonal ensemble, and the GGE based on all known local conserved charges. We display these differences explicitly for short-distance spin-spin correlations and verify them using NLCE. Our results highlight how far-from-equilibrium dynamics can reveal the effects of physically relevant but unknown conserved quantities in interacting integrable models.

Quench protocol.—Our initial state is the ground state of the antiferromagnetic Ising model, namely, the translationally invariant Néel state

$$|\Psi_0\rangle = \frac{1}{\sqrt{2}}(|\uparrow\downarrow\uparrow\downarrow\ldots\rangle + |\downarrow\uparrow\downarrow\uparrow\ldots\rangle). \tag{1}$$

The time evolution after the quench is governed by the antiferromagnetic XXZ spin chain Hamiltonian

$$H = \frac{J}{4}\sum_{j=1}^{N}[\sigma_j^x\sigma_{j+1}^x + \sigma_j^y\sigma_{j+1}^y + \Delta(\sigma_j^z\sigma_{j+1}^z - 1)], \tag{2}$$

with exchange coupling $J > 0$. The Néel state is the ground state in the limit $\Delta \to \infty$. The Pauli matrices σ_j^α

($\alpha = x, y, z$) represent the spin-1/2 degrees of freedom at lattice sites $j = 1, 2, \ldots, N$, and we assume periodic boundary conditions $\sigma^{\alpha}_{N+1} = \sigma^{\alpha}_{1}$. We restrict our analysis to quenches for which $\Delta \geq 1$ (details for the $\Delta = 1$ case are provided in Ref. [52]).

Eigenstates of the Hamiltonian (2) can be obtained by Bethe ansatz [53,54]. Each normalized Bethe wave function

$$|\boldsymbol{\lambda}\rangle = \sum_{\mathbf{x}} \sum_{Q} A_{Q}(\boldsymbol{\lambda}) \prod_{j=1}^{M} e^{i x_j p(\lambda_{Q_j})} \sigma^{-}_{x_j} |\uparrow\uparrow \ldots \uparrow\rangle \qquad (3)$$

lies in a fixed magnetization sector $\langle \sigma^{z}_{\mathrm{tot}} \rangle / 2 = N/2 - M$. It is completely specified by a set of complex quasimomenta or rapidities $\boldsymbol{\lambda} = \{\lambda_k\}_{k=1}^{M}$, which satisfy the Bethe equations

$$\left(\frac{\sin(\lambda_j + i\eta/2)}{\sin(\lambda_j - i\eta/2)} \right)^{N} = - \prod_{k=1}^{M} \frac{\sin(\lambda_j - \lambda_k + i\eta)}{\sin(\lambda_j - \lambda_k - i\eta)}, \qquad (4)$$

for $j = 1, \ldots, M$. The parameter $\eta > 0$ is related to the anisotropy parameter $\Delta = \cosh(\eta)$. The first sum in Eq. (3) is over all ordered configurations $\mathbf{x} = \{x_j\}_{j=1}^{M} \subset \{1, \ldots, N\}$ of down spin positions, while the second sum runs over all permutations Q of labels $\{1, \ldots, M\}$. $A_Q(\boldsymbol{\lambda})$ are rapidity-dependent amplitudes [53,54]. The total momentum and energy of a Bethe state are given by

$$P_{\boldsymbol{\lambda}} = \sum_{j=1}^{M} p(\lambda_j), \qquad p(\lambda) = i \ln \left[\frac{\sin(\lambda - i\eta/2)}{\sin(\lambda + i\eta/2)} \right], \qquad (5)$$

$$\omega_{\boldsymbol{\lambda}} = \sum_{j=1}^{M} e(\lambda_j), \qquad e(\lambda) = -J\pi \sinh(\eta) a_1(\lambda), \qquad (6)$$

where $a_1(\lambda) = \sinh(\eta)/[\pi(\cosh\eta - \cos 2\lambda)]$.

Bethe states are classified according to the string hypothesis [53,55]. Rapidities arrange themselves in strings $\lambda^{n,a}_{\alpha} = \lambda^{n}_{\alpha} + (i\eta/2)(n+1-2a) + i\delta^{n,a}_{\alpha}$, $a = 1, \ldots, n$, where n is the length of the string and the deviations $\delta^{n,a}_{\alpha}$ vanish (typically exponentially) upon taking the infinite-size limit. For $\Delta > 1$, the string centers λ^{n}_{α} lie in the interval $[-\pi/2, \pi/2)$. Physically, such an n-string corresponds to a bound state of n magnons, which in the Ising limit $\Delta \to \infty$ can be seen as a block of n adjacent down spins.

At time t after the quench, the state of the system can be expanded in the basis of Bethe states such that the postquench time-dependent expectation value of a generic operator $\mathcal{O}$ is exactly given by the double sum

$$\langle \Psi(t)|\mathcal{O}|\Psi(t)\rangle = \sum_{\boldsymbol{\lambda},\boldsymbol{\lambda}'} e^{-S^{*}_{\boldsymbol{\lambda}} - S_{\boldsymbol{\lambda}'}} e^{i(\omega_{\boldsymbol{\lambda}} - \omega_{\boldsymbol{\lambda}'})t} \langle \boldsymbol{\lambda}|\mathcal{O}|\boldsymbol{\lambda}'\rangle, \qquad (7)$$

with overlap coefficients $S_{\boldsymbol{\lambda}} = -\ln \langle \boldsymbol{\lambda}|\Psi_0\rangle$.

Quench action.—The double sum over the full Hilbert space in Eq. (7) represents a substantial bottleneck, its size growing exponentially with N. The quench-action method [48,51] gives a handle on this double sum in the thermodynamic limit $N \to \infty$ (with $M/N = 1/2$ fixed), denoted by $\lim_{\mathrm{th}}$. In this limit, a state is characterized by the distributions of its string centers. They are given by a set of positive, smooth, and bounded densities $\boldsymbol{\rho} = \{\rho_n\}_{n=1}^{\infty}$ for the string centers λ^{n}_{α}, representing a set of Bethe states with Yang-Yang (YY) entropy

$$\frac{S_{\mathrm{YY}}[\boldsymbol{\rho}]}{N} = \sum_{n=1}^{\infty} \int_{-\pi/2}^{\pi/2} d\lambda [\rho_n \ln(1+\eta_n) + \rho_{n,h} \ln(1+\eta_n^{-1})]. \qquad (8)$$

Here, $\rho_{n,h}$ is the density of holes of n-string centers [56,57], $\eta_n = \rho_{n,h}/\rho_n$, and we leave the λ dependence implicit. The Bethe Eqs. (4) become a set of coupled integral equations [55] for the densities $\boldsymbol{\rho}$,

$$\rho_n(1+\eta_n) = s * (\eta_{n-1}\rho_{n-1} + \eta_{n+1}\rho_{n+1}), \qquad n \geq 1, \quad (9)$$

with $\eta_0(\lambda) = 1$ and $\rho_0(\lambda) = \delta(\lambda)$. The convolution $*$ is defined by $(f * g)(\lambda) = \int_{-\pi/2}^{\pi/2} f(\lambda - \mu) g(\mu) d\mu$, and the kernel in Eqs. (9) is $s(\lambda) = (2\pi)^{-1} \sum_{k \in \mathbb{Z}} [e^{-2ik\lambda}/\cosh(k\eta)]$.

As explained in Ref. [51], for a large class of physical observables, the double sum in Eq. (7) can be recast in the thermodynamic limit as a functional integral over the root densities $\boldsymbol{\rho}$. The weight of the functional integral $e^{-S_{\mathrm{QA}}[\boldsymbol{\rho}]}$ is given by the quench action (QA) $S_{\mathrm{QA}}[\boldsymbol{\rho}] = 2S[\boldsymbol{\rho}] - S_{\mathrm{YY}}[\boldsymbol{\rho}]$, where $S[\boldsymbol{\rho}] = \lim_{\mathrm{th}} \mathrm{Re} S_{\boldsymbol{\lambda}}$ is the extensive real part of the overlap coefficient in the thermodynamic limit. Since the quench action is extensive, real, and bounded from below, a saddle-point (sp) approximation becomes exact in the thermodynamic limit. At long times after the quench, the system relaxes to a steady state $\boldsymbol{\rho}^{\mathrm{sp}}$ determined by the variational equations

$$0 = \left. \frac{\delta S_{\mathrm{QA}}[\boldsymbol{\rho}]}{\delta \rho_n(\lambda)} \right|_{\boldsymbol{\rho} = \boldsymbol{\rho}^{\mathrm{sp}}} \quad \text{for } n \geq 1. \qquad (10)$$

Steady-state expectation values of physical observables can then be effectively computed on this state,

$$\lim_{t \to \infty} \lim_{\mathrm{th}} \langle \Psi(t)|\mathcal{O}|\Psi(t)\rangle = \langle \boldsymbol{\rho}^{\mathrm{sp}}|\mathcal{O}|\boldsymbol{\rho}^{\mathrm{sp}}\rangle. \qquad (11)$$

The saddle-point distributions of string centers $\boldsymbol{\rho}^{\mathrm{sp}}$ thus encode all equilibrium expectation values and correlators of physical observables after the quench [14,48].

The implementation of the quench action approach to the Néel-to-XXZ quench proceeds as follows (see the Supplemental Material [58] for details). One of the main ingredients is the leading-order behavior of the overlaps $\langle \boldsymbol{\lambda}|\Psi_0\rangle$ in the thermodynamic limit. It was proven in Refs. [59,60] (starting from Refs. [61,62]) that only overlaps between $|\Psi_0\rangle$ and parity-invariant Bethe states are

nonvanishing; practical determinant expressions were also derived. Taking M to be even, rapidities of parity-invariant states come in pairs such that $\{\lambda_j\}_{j=1}^{M} = \{-\lambda_j\}_{j=1}^{M}$ and the overlap is now determined by $M/2$ rapidities $\tilde{\boldsymbol{\lambda}} = \{\lambda_j\}_{j=1}^{M/2}$. The overlap's leading term (in system size) reads [59]

$$\langle \tilde{\boldsymbol{\lambda}} | \Psi_0 \rangle \sim \prod_{j=1}^{M/2} \frac{\sqrt{\tan(\lambda_j + i\eta/2)\tan(\lambda_j - i\eta/2)}}{2\sin(2\lambda_j)}. \quad (12)$$

One can straightforwardly separate the contributions of different string lengths and derive an expression for the thermodynamic overlap coefficients $S[\boldsymbol{\rho}]$. Before varying the quench action, per Eqs. (10), one needs to add a Lagrange multiplier fixing the filling of the saddle-point state to the Néel state's $\lim_{\text{th}} M/N = 1/2$. Variation leads to a set of generalized thermodynamic Bethe ansatz (GTBA) equations for the functions η_n (see the Supplemental Material [58]),

$$\ln(\eta_n) = d_n + s * [\ln(1+\eta_{n-1}) + \ln(1+\eta_{n+1})], \quad (13)$$

where $n \geq 1$, $\eta_0(\lambda) = 0$ by convention, and

$$d_n(\lambda) = \sum_{k\in\mathbb{Z}} e^{-2ik\lambda} \frac{\tanh(\eta k)}{k} [(-1)^n - (-1)^k]. \quad (14)$$

The solution to the GTBA Eqs. (13), substituted into the Bethe Eqs. (9), leads to a set of root densities $\boldsymbol{\rho}^{\text{sp}}$ describing the steady state of the Néel-to-XXZ quench. They can be numerically computed by truncating the infinite sets of Eqs. (13) and (9). In Figs. 1(a) and 1(b), we plot saddle-point distributions of 1- and 2-strings for different values of Δ. A notable feature is the vanishing of the even-length string densities at $\lambda = 0$, which corresponds to the fact that the overlaps (12) between the Néel state and parity-invariant Bethe states with a string of even length centered at zero identically vanish. Furthermore, for large Δ values, the density of 1-strings becomes increasingly dominant, approaching the ground state of the Ising model [$\rho_1(\lambda) = 1/(2\pi)$ and $\rho_n(\lambda) = 0$ for $n \geq 2$], in accordance with the expected result for the quenchless point $\Delta = \infty$.

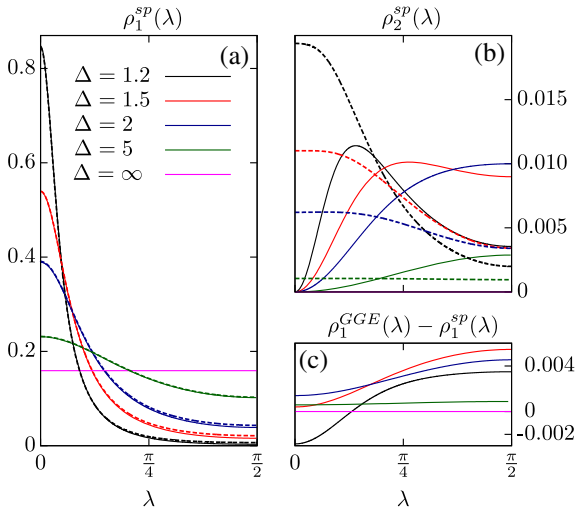

FIG. 1 (color online). (a),(b) Density functions ρ_1 and ρ_2 for the quench to different values of $\Delta > 1$ of both the quench-action saddle-point state (solid lines) and the GGE equilibrium state (dashed lines). (c) Difference between the GGE prediction for ρ_1 and the quench-action saddle-point result. All distributions are symmetric functions of $\lambda \in [-\pi/2, \pi/2)$.

NLCE.—Our NLCE follows on Ref. [49] and has been tailored to solve the specific quench studied in this work [50,58]. NLCEs enable the calculation of the infinite-time average (also known as the diagonal ensemble result) of correlation functions after the quench in the thermodynamic limit [49,50]. The idea is that any spin-spin correlation can be computed as a sum over the contributions from all connected clusters c that can be embedded on the lattice, $\langle \sigma_i^z \sigma_j^z \rangle_{\text{NLCE}} = \sum_c M(c) \times \mathcal{W}_{\sigma_i^z\sigma_j^z}(c)$, where $M(c)$ is the number of embeddings of c per site, and $\mathcal{W}_{\sigma_i^z\sigma_j^z}(c)$ is the weight of $\sigma_i^z\sigma_j^z$ in c. The latter is calculated using the inclusion-exclusion principle $\mathcal{W}_{\sigma_i^z\sigma_j^z}(c) = \langle \sigma_i^z\sigma_j^z \rangle_c^{\text{DE}} - \sum_{s\subset c} \mathcal{W}_{\sigma_i^z\sigma_j^z}(s)$, where the last sum runs over all connected subclusters of c, and $\langle \sigma_i^z\sigma_j^z \rangle_c^{\text{DE}} = \text{Tr}[\sigma_i^z\sigma_j^z\hat{\rho}_c^{\text{DE}}]/\text{Tr}[\hat{\rho}_c^{\text{DE}}]$ is the expectation value of $\sigma_i^z\sigma_j^z$ calculated with the density matrix in the diagonal ensemble (DE) $\hat{\rho}_c^{\text{DE}}$ (in cluster c). In order to accelerate the convergence of the NLCE, we use Wynn's and Brezinski's resummation algorithms (Supplemental Material [58]) [63,64].

GGE.—The integrable structure of the XXZ spin chain provides, in the thermodynamic limit, an infinite set of local conserved charges Q_m, $m \in \mathbb{N}$, such that $Q_1 \propto P$, $Q_2 \propto H$ [65,66]. For integrable models, it is conjectured (and shown for specific quenches) that the steady state after a quench can be described by a GGE. For the XXZ spin chain, the latter is given by a set of densities $\boldsymbol{\rho}^{\text{GGE}}$ that maximizes the Yang-Yang entropy $S_{\text{YY}}[\boldsymbol{\rho}]$ under the constraint of fixed expectation values of the local conserved charges Q_m [67,68]. This translates into GTBA equations of the same form as Eqs. (13) but now with the driving function d_1 determined by the chemical potentials associated with the charges and the remaining $d_n(\lambda) = 0$ for $n \geq 2$. Together with Eqs. (9), this uniquely determines $\boldsymbol{\rho}^{\text{GGE}}$. In general, the values of the chemical potentials are inaccessible for the XXZ model, except for a truncated GGE when only a small number of conserved charges is taken into account [36].

However, it turns out that the expectation values of all local conserved charges Q_m on the initial state are in one-to-one correspondence with the density $\rho_{1,h}$ of 1-string holes, i.e.,

$$\lim_{\text{th}} \left(\frac{\langle \Psi_0 | Q_{2m+2} | \Psi_0 \rangle}{N \sinh^{2m+1}(\eta)} \right) = \sum_{k\in\mathbb{Z}} \frac{\hat{\rho}_{1,h}(k) - e^{-|k|\eta}}{2\cosh(k\eta)} (ik)^{2m}, \quad (15)$$

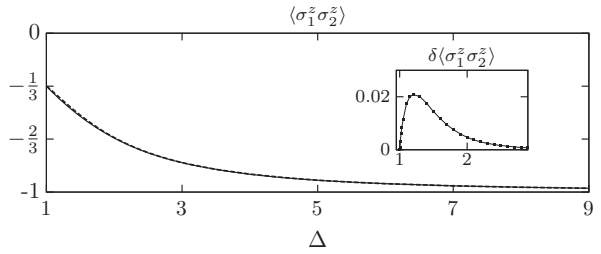

FIG. 2. Correlator $\langle\sigma_1^z\sigma_2^z\rangle$ evaluated on the quench-action steady state (solid lines) and on the GGE (dashed lines). The energy sum rule $2\langle\sigma_1^x\sigma_2^x\rangle + \Delta\langle\sigma_1^z\sigma_2^z\rangle = -\Delta$ explains the exact value of $-1/3$ at the isotropic point $\Delta = 1$. Numerical errors are 10^{-5} or smaller. Both sets of data are in agreement with the finite-size computations of Ref. [19], within the numerical precision of the latter. Inset: Relative difference between the GGE prediction and the quench-action saddle-point result, $\delta\langle\sigma_1^z\sigma_2^z\rangle = (\langle\sigma_1^z\sigma_2^z\rangle_{\mathrm{GGE}} - \langle\sigma_1^z\sigma_2^z\rangle_{\mathrm{sp}})/|\langle\sigma_1^z\sigma_2^z\rangle_{\mathrm{sp}}|$.

with $m \geq 0$ and $\hat{\rho}_{1,h}$ the Fourier transform of $\rho_{1,h}$, see the Supplemental Material [58]. In the case of the Néel-to-XXZ quench, the expectation values of the conserved charges on the initial state [69] fix $\rho_{1,h}$ unambiguously [52],

$$\rho_{1,h}^{\mathrm{Néel}}(\lambda) = \frac{\pi^2 a_1^3(\lambda)\sin^2(2\lambda)}{\pi^2 a_1^2(\lambda)\sin^2(2\lambda) + \cosh^2(\eta)}, \qquad (16)$$

where a_1 was defined right after Eq. (6). This makes the input from the chemical potentials redundant. The densities $\boldsymbol{\rho}^{\mathrm{GGE}}$ for the GGE can be found by solving the GTBA Eqs. (13) for $n \geq 2$ [$d_n(\lambda) = 0$] and the Bethe Eqs. (9) with the constraint $\rho_{1,h}^{\mathrm{GGE}} = \rho_{1,h}^{\mathrm{Néel}}$.

Discussion of results.—Numerical and analytical analysis show exact agreement between $\rho_{1,h}$ predicted by the quench-action approach and $\rho_{1,h}^{\mathrm{Néel}}$ in Eq. (16) [52]. The expectation values of all local conserved charges Q_n are, thus, reproduced exactly. We stress that this nontrivial agreement constitutes strong evidence for the correctness of the quench-action prediction of the steady state.

Furthermore, the distributions of the GGE can be compared with the steady-state distributions provided by the quench-action approach, see Fig. 1. The densities ρ_n for the GGE and the quench action are clearly different, the discrepancies becoming more pronounced as one reduces the anisotropy towards the gapless point $\Delta = 1$. We emphasize that all our results are obtained in the thermodynamic limit: these differences are not finite-size effects.

We verified the existence of these discrepancies by analytically solving the GTBA equations of the two ensembles in a large-Δ expansion. The differences between the distributions are of order Δ^{-2}, e.g., for 1- and 2-strings (for other strings and higher orders, see Ref. [52])

$$\rho_1^{\mathrm{GGE}}(\lambda) - \rho_1^{\mathrm{sp}}(\lambda) = \frac{1}{4\pi\Delta^2} + O(\Delta^{-3}), \qquad (17a)$$

$$\rho_2^{\mathrm{GGE}}(\lambda) - \rho_2^{\mathrm{sp}}(\lambda) = \frac{1 - 3\sin^2(\lambda)}{3\pi\Delta^2} + O(\Delta^{-3}). \qquad (17b)$$

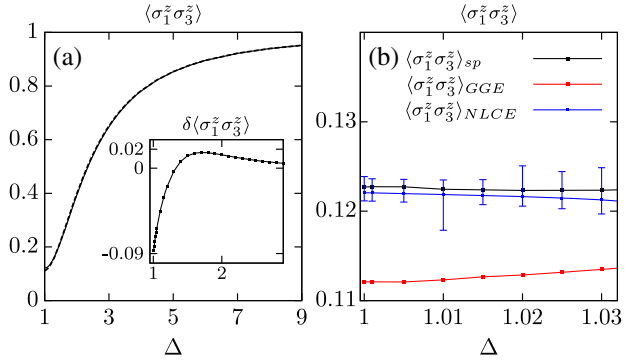

FIG. 3 (color online). (a) The same as Fig. 2 for $\langle\sigma_1^z\sigma_3^z\rangle$. (b) Comparison between the quench action, the GGE prediction, and the NLCE result close to the isotropic point. Error bars in the NLCE data display an interval of confidence that includes all resummation results (except for $\Delta = 1.015$) (Supplemental Material [58]).

Given steady-state distributions, one can compute physical observables [Eq. (11)]. Nonvanishing differences between distributions will generally be reflected in those expectation values, even in simple ones such as few-point spin-spin correlation functions. We have implemented an adapted version of the Hellmann-Feynman theorem to compute the expectation value $\langle\sigma_1^z\sigma_2^z\rangle$ from the distributions $\boldsymbol{\rho}$ [58,70]. The nearest-neighbor two-point correlator is predicted differently by the quench-action steady state and the GGE (see Fig. 2). The NLCE results (not shown) are consistent with those predictions but cannot resolve their difference since it is too small ($\lesssim 2\%$, as shown in the inset in Fig. 2). It should be noted that the magnitude of differences between distributions in Eqs. (17) does not directly translate into a similar difference for physical observables. Expanding for large anisotropy, we obtain a discrepancy of order Δ^{-6},

$$\langle\sigma_1^z\sigma_2^z\rangle_{\mathrm{GGE}} - \langle\sigma_1^z\sigma_2^z\rangle_{\mathrm{sp}} = \frac{9}{16\Delta^6} + O(\Delta^{-7}). \qquad (18)$$

We also calculate the next-nearest-neighbor correlator $\langle\sigma_1^z\sigma_3^z\rangle$ by means of the method of Ref. [70], see Fig. 3. In the inset in Fig. 3(a) one can see that, as $\Delta \to 1$, the differences between the predictions of the quench-action approach and the GGE become of the order of 10%. Figure 3(b) provides a closer look of $\langle\sigma_1^z\sigma_3^z\rangle$ in that regime. There, we also report our NLCE results (Supplemental Material [58]). The latter are consistent with the quench-action predictions and inconsistent with the GGE results. Hence, our NLCE calculations support the correctness of the QA approach for describing observables after relaxation and the inability of the GGE constructed here to do so.

Conclusions.—We used the quench-action method to obtain an exact description of the steady state following a quench from the ground state of the Ising model to an XXZ spin-1/2 chain with anisotropy $\Delta \geq 1$. We were also able to

fully implement a GGE based on all known local conserved charges. Our main finding is that the quench-action steady state is different from the GGE prediction. We have shown that even for local correlators, the methods produce different results. An independent NLCE calculation supports the predictions of the quench-action approach. A possible interpretation of our results is that GGE based on the local charges Q_m is incomplete and that a larger set of conserved (quasi- or nonlocal) charges is needed [71–73]. This makes it apparent that the study of quantum quenches provides a unique venue to further deepen our understanding of interacting integrable models.

It also remains an interesting open problem to extend our results to the gapless regime $-1 < \Delta < 1$ and, going beyond steady-state issues, to reconstruct the postquench time-dependent relaxation itself, which is accessible via a quench-action treatment and which would make correspondence to eventual experimental realizations more direct. We will return to these and further applications of the quench-action method in future work.

We would like to thank P. Calabrese, F. Essler, M. Fagotti, F. Göhmann, V. Gritsev, A. Klümper, R. Konik, M. Kormos, B. Pozsgay, and R. Vlijm for useful discussions. We acknowledge support from the Foundation for Fundamental Research on Matter (FOM), the Netherlands Organisation for Scientific Research (NWO), and the U.S. Office of Naval Research. For their support and hospitality, M. B., M. R., and J.-S. C. thank the Perimeter Institute, and B. W., J. D. N. and J.-S. C. thank CUNY (where the main results of this work were first made public). This work forms part of the activities of the Delta Institute for Theoretical Physics (D-ITP).

Note added.—Further evidence that, in contrast to the GGE, the quench-action approach correctly predicts the steady state for XXZ quenches is presented in the accompanying Letter [74]. Related issues are also treated in two other recent papers [75,76].

[1] T. Kibble, Phys. Rep. **67**, 183 (1980).
[2] W. Zurek, Nature (London) **317**, 505 (1985).
[3] G. D. Moore and D. Teaney, Phys. Rev. C **71**, 064904 (2005).
[4] M. C. Cross and P. C. Hohenberg, Rev. Mod. Phys. **65**, 851 (1993).
[5] T. Chou, K. Mallick, and R. K. P. Zia, Rep. Prog. Phys. **74**, 116601 (2011).
[6] J. Kurchan, Nature (London) **433**, 222 (2005).
[7] A. Polkovnikov, K. Sengupta, A. Silva, and M. Vengalattore, Rev. Mod. Phys. **83**, 863 (2011).
[8] P. Calabrese and J. Cardy, Phys. Rev. Lett. **96**, 136801 (2006).
[9] M. Rigol, V. Dunjko, V. Yurovsky, and M. Olshanii, Phys. Rev. Lett. **98**, 050405 (2007).
[10] M. Rigol, A. Muramatsu, and M. Olshanii, Phys. Rev. A **74**, 053616 (2006).
[11] M. Rigol, V. Dunjko, and M. Olshanii, Nature (London) **452**, 854 (2008).
[12] T. Barthel and U. Schollwöck, Phys. Rev. Lett. **100**, 100601 (2008).
[13] M. Cramer and J. Eisert, New J. Phys. **12**, 055020 (2010).
[14] A. C. Cassidy, C. W. Clark, and M. Rigol, Phys. Rev. Lett. **106**, 140405 (2011).
[15] P. Calabrese, F. H. L. Essler, and M. Fagotti, Phys. Rev. Lett. **106**, 227203 (2011).
[16] P. Calabrese, F. H. L. Essler, and M. Fagotti, J. Stat. Mech. (2012) P07016.
[17] P. Calabrese, F. H. L. Essler, and M. Fagotti, J. Stat. Mech. (2012) P07022.
[18] B. Pozsgay, J. Stat. Mech. (2013) P07003.
[19] M. Fagotti, M. Collura, F. H. L. Essler, and P. Calabrese, Phys. Rev. B **89**, 125101 (2014).
[20] L. Bucciantini, M. Kormos, and P. Calabrese, J. Phys. A **47**, 175002 (2014).
[21] P. Barmettler, M. Punk, V. Gritsev, E. Demler, and E. Altman, Phys. Rev. Lett. **102**, 130603 (2009).
[22] P. Barmettler, M. Punk, V. Gritsev, E. Demler, and E. Altman, New J. Phys. **12**, 055017 (2010).
[23] D. Rossini, A. Silva, G. Mussardo, and G. E. Santoro, Phys. Rev. Lett. **102**, 127204 (2009).
[24] D. Rossini, S. Suzuki, G. Mussardo, G. E. Santoro, and A. Silva, Phys. Rev. B **82**, 144302 (2010).
[25] A. Faribault, P. Calabrese, and J.-S. Caux, J. Math. Phys. (N.Y.) **50**, 095212 (2009).
[26] J. Mossel and J.-S. Caux, New J. Phys. **12**, 055028 (2010).
[27] F. Iglói and H. Rieger, Phys. Rev. Lett. **106**, 035701 (2011).
[28] M. C. Bañuls, J. I. Cirac, and M. B. Hastings, Phys. Rev. Lett. **106**, 050405 (2011).
[29] W. Liu and N. Andrei, Phys. Rev. Lett. **112**, 257204 (2014).
[30] M. Rigol and M. Fitzpatrick, Phys. Rev. A **84**, 033640 (2011).
[31] G. P. Brandino, A. De Luca, R. M. Konik, and G. Mussardo, Phys. Rev. B **85**, 214435 (2012).
[32] E. Demler and A. M. Tsvelik, Phys. Rev. B **86**, 115448 (2012).
[33] K. He and M. Rigol, Phys. Rev. A **85**, 063609 (2012).
[34] K. He and M. Rigol, Phys. Rev. A **87**, 043615 (2013).
[35] M. Heyl, A. Polkovnikov, and S. Kehrein, Phys. Rev. Lett. **110**, 135704 (2013).
[36] B. Pozsgay, J. Stat. Mech. (2013) P10028.
[37] M. Fagotti, arXiv:1308.0277.
[38] M. Heyl, arXiv:1403.4570.
[39] M. Marcuzzi, J. Marino, A. Gambassi, and A. Silva, Phys. Rev. Lett. **111**, 197203 (2013).
[40] G. Mussardo, Phys. Rev. Lett. **111**, 100401 (2013).
[41] M. Kormos, A. Shashi, Y.-Z. Chou, J.-S. Caux, and A. Imambekov, Phys. Rev. B **88**, 205131 (2013).
[42] F. H. L. Essler, S. Kehrein, S. R. Manmana, and N. J. Robinson, Phys. Rev. B **89**, 165104 (2014).
[43] T. Kinoshita, T. Wenger, and D. S. Weiss, Nature (London) **440**, 900 (2006).
[44] S. Trotzky, Y.-A. Chen, A. Flesch, I. P. McCulloch, U. Schollwöck, J. Eisert, and I. Bloch, Nat. Phys. **8**, 325 (2012).
[45] M. Cheneau, P. Barmettler, D. Poletti, M. Endres, P. Schauss, T. Fukuhara, C. Gross, I. Bloch, C. Kollath, and S. Kuhr, Nature (London) **481**, 484 (2012).

[46] M. Gring, M. Kuhnert, T. Langen, T. Kitagawa, B. Rauer, M. Schreitl, I. Mazets, D. A. Smith, E. Demler, and J. Schmiedmayer, Science **337**, 1318 (2012).
[47] T. Fukuhara, P. Schauss, M. Endres, S. Hild, M. Cheneau, I. Bloch, and C. Gross, Nature (London) **502**, 76 (2013).
[48] J.-S. Caux and F. H. L. Essler, Phys. Rev. Lett. **110**, 257203 (2013).
[49] M. Rigol, Phys. Rev. Lett. **112**, 170601 (2014).
[50] M. Rigol, arXiv:1407.6357.
[51] J. De Nardis, B. Wouters, M. Brockmann, and J.-S. Caux, Phys. Rev. A **89**, 033601 (2014).
[52] M. Brockmann, B. Wouters, D. Fioretto, J. De Nardis, R. Vlijm, and J.-S. Caux, arXiv:1408.5075.
[53] H. Bethe, Z. Phys. **71**, 205 (1931).
[54] R. Orbach, Phys. Rev. **112**, 309 (1958).
[55] M. Takahashi, Prog. Theor. Phys. **46**, 401 (1971).
[56] V. E. Korepin, N. M. Bogoliubov, and A. G. Izergin, *Quantum Inverse Scattering Method and Correlation Functions* (Cambridge University Press, Cambridge, England, 1993).
[57] M. Takahashi, *Thermodynamics of One-Dimensional Solvable Models* (Cambridge University Press, Cambridge, England, 1999).
[58] See the Supplemental Material at http://link.aps.org/supplemental/10.1103/PhysRevLett.113.117202 for the derivation of the GTBA equations, as well as the computation of the nearest-neighbor correlator and the NLCE implementation.
[59] M. Brockmann, J. De Nardis, B. Wouters, and J.-S. Caux, J. Phys. A **47**, 145003 (2014).
[60] M. Brockmann, J. De Nardis, B. Wouters, and J.-S. Caux, J. Phys. A **47**, 345003 (2014).
[61] O. Tsuchiya, J. Math. Phys. (N.Y.) **39**, 5946 (1998).
[62] K. K. Kozlowski and B. Pozsgay, J. Stat. Mech. (2012) P05021.
[63] M. Rigol, T. Bryant, and R. R. P. Singh, Phys. Rev. Lett. **97**, 187202 (2006).
[64] M. Rigol, T. Bryant, and R. R. P. Singh, Phys. Rev. E **75**, 061118 (2007).
[65] M. P. Grabowski and P. Mathieu, Mod. Phys. Lett. A **09**, 2197 (1994).
[66] M. P. Grabowski and P. Mathieu, Ann. Phys. (N.Y.) **243**, 299 (1995).
[67] J. Mossel and J.-S. Caux, J. Phys. A **45**, 255001 (2012).
[68] J.-S. Caux and R. M. Konik, Phys. Rev. Lett. **109**, 175301 (2012).
[69] M. Fagotti and F. H. L. Essler, J. Stat. Mech. (2013) P07012.
[70] M. Mestyan and B. Pozsgay, arXiv:1405.0232.
[71] T. Prosen, Phys. Rev. Lett. **106**, 217206 (2011).
[72] T. Prosen, arXiv:1406.2258.
[73] R. G. Pereira, V. Pasquier, J. Sirker, and I. Affleck, arXiv:1406.2306.
[74] B. Pozsgay, M. Mestyán, M. A. Werner, M. Kormos, G. Zaránd, and G. Takács, following Letter, Phys Rev. Lett. **113**, 117203 (2014).
[75] G. Goldstein and N. Andrei, arXiv:1405.4224 [Phys. Rev. A (to be published)].
[76] B. Pozsgay, arXiv:1406.4613.